CHEMISTRY
A European Journal

A Journal of
ChemPubSoc Europe

Accepted Article

Title: 2-(Hydroxyimino)aldehydes: Photochemical and Physico-Chemical Properties of a versatile functional group for monomer design

Authors: Patrizia Gentili, Martina Nardi, Irene Antignano, Paolo Cambise, Marco D'Abramo, Francesca D'Acunzo, Alessandro Pinna, and Emanuele Ussia

To be cited as: *Chem. Eur. J.* 10.1002/chem.201800059

Link to VoR: http://dx.doi.org/10.1002/chem.201800059

Supported by
ACES

WILEY-VCH

10.1002/chem.201800059

WILEY-VCH

2-(Hydroxyimino)aldehydes: Photochemical and Physico-Chemical Properties of a versatile functional group for monomer design

Patrizia Gentili*[ab], Martina Nardi[ab], Irene Antignano[a], Paolo Cambise[a], Marco D'Abramo[a], Francesca D'Acunzo*[b], Alessandro Pinna[a], Emanuele Ussia[a]

Abstract: In the context of our research on stimuli-responsive polymers bearing the 2-(hydroxyimino)aldehyde (HIA) group, we explore the photochemical behavior and physico-chemical properties of a number of HIAs. Interpretation of experimental data is supported by quantum mechanical calculations. HIAs are expected to undergo photoisomerization, chelate metal ions, yield hydrogen-bonded dimers or oligomers, exhibit relatively low pK_as, and form >C=NO• radicals through OH hydrogen abstraction or oxidation of the oximate ion. Besides the well-established *E*/*Z* oxime photoisomerism, we observe a Norrish-Yang cyclization resulting in cyclobutanol oximes, to our knowledge not described in previous literature. Acidity, Bond Dissociation Enthalpies and electrochemical properties of HIAs are compared to literature data on simple oximes. Results are discussed in relation to the many potential applications for HIAs, with emphasis on the synthesis of novel HIA-containing responsive polymers.

Introduction

2-(hydroxyimino)aldehydes (HIAs; Figure 1a) are a class of organic compounds that has been sporadically investigated in the scientific literature, mainly in the context of organic synthesis. Convenient methods for the synthesis of 2-(hydroxyimino)carbonyl compounds are being continuously proposed: Sugamoto[2] resorted to reduction-nitrosation with *t*-butyl nitrite and triethylsilane in the presence of cobalt(II) porphyrin as a catalyst; 3-chloro-2-hydroxyiminopropanal (Figure 1: R=CH_2Cl) was prepared by Gilchrist and Roberts by addition of nitrosyl chloride to acrylaldehyde at low temperature;[3] Baidya and Yamamoto[4] obtained several HIAs through oxidation of the corresponding aldehydes with aluminum nitrite. Finally, a convenient α-oximation reaction of aldehydes has been developed in our laboratory,[5] which affords good to excellent yields of HIAs via organo-SOMO catalysis. This reaction affords HIAs bearing substituents of different bulk and nature (Figure 1), so that a systematic investigation of their physico-chemical properties is now accessible. Oximes in general are highly versatile molecules and HIAs may exhibit yet more interesting properties, thanks to the presence of an oxime and aldehyde group in adjacent position.

Oximes are building blocks for the synthesis of heterocyclic compounds,[6] they can exhibit biological activity,[7] and they can be used as handles for bioorthogonal conjugation[8] through the formation of oxime ether bonds.[9] In this context, HIAs, which carry a combination of electrophilic (CHO and C=NOH) and nucleophilic sites (oxime N and O) can be viewed as multi-functional platforms for bioconjugation. Oximate ions are of interest for the decontamination from toxic metal ions[10] or from organophosphorous compounds.[11] Oximes are known to exist in two configurations, where the residue with the highest priority is either *E* or *Z* with respect to the oxime OH group. The photo-induced switch of the *E*/*Z* configuration in imines, oximes and hydrazones has been extensively investigated in the field of light-driven molecular machines (see Ref[12] and references therein). In the case of HIAs, the aldehyde group has the highest priority, so that *E*/*Z* isomerism is referred to the relative positions of the oxime OH and aldehyde groups about the oxime double bond (Figure 1a). The interaction

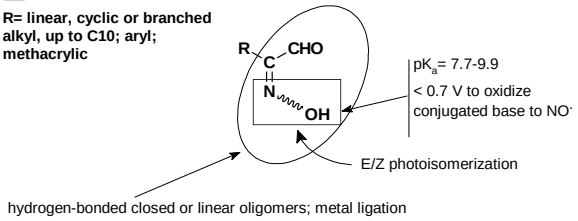

a) 2-(hydroxyimino)aldehydes (HIAs)

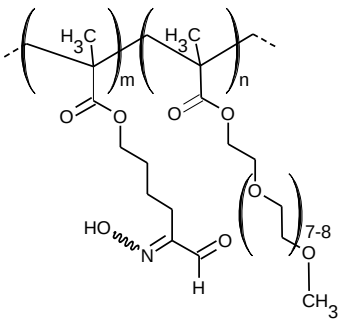

b) poly(HIAMBA-*co*-OEGMA$_{475}$)

Figure 1. a) General structure and properties of 2-(hydroxyimino)aldehydes (HIAs); **b)** Structure of poly(HIAMBA-*co*-OEGMA$_{475}$), an HIA-containing copolymer from our recent investigation.[1] HIABMA= 4-[(hydroxyimino)aldehyde]butyl methacrylate

[a] Prof. P Gentili, Dr. M Nardi, I Antignano, Dr. P Cambise, Prof. M D'Abramo, Dr. A Pinna, Dr. E Ussia
Dipartimento di Chimica, Università degli Studi "La Sapienza" P.le A. Moro 5, 00185 Rome, Italy
E-mail: patrizia.gentili@uniroma1.it
[b] Prof. P Gentili, Dr. M Nardi,, Dr. F D'Acunzo
CNR, Istituto di Metodologie Chimiche, Sezione Meccanismi di Reazione c/o Dipartimento di Chimica,Università degli Studi "La Sapienza" P.le A. Moro 5, 00185 Roma, Italy.
E-mail: francesca.dacunzo@uniroma1.it
Supporting information for this article is given via a link at the end of the document.

between the adjacent aldehyde and oxime groups in HIAs, mainly in terms of hydrogen bonding and conjugation of the oximate anion, is likely to be different in the two configurations, thus resulting in distinct physico-chemical properties. Such interaction, which is also influenced by the nature and bulk of the R group, has been studied in the case of other 2-substituted oximes, such as α-keto-oximes,[13] monoterpenoid oximes,[14] pyrrole-2-carbaldehyde oxime,[15] nitrosation products of phosphorylaldehydes[16] and α-cyanoximes.[17] HIAs are expected to possess a lower pKa than the corresponding unsubstituted oximes, so that it is of paramount importance to determine their acidity in view of possible applications where oximate ions are involved. Knowledge of the redox properties and UV-Vis absorption of HIAs is also relevant towards other technological applications, as in Dye-Sensitized Solar Cells, in which they may serve either as sensitizing dyes, or as iodine-free shuttle systems.[18] In this context, the configurational behavior of HIAs upon exposure to light is likely to be coupled with the physico-chemical properties of these molecules and of their metal complexes. In fact, the ability of oximes to form dimers, trimers, tetramers or catamers has been associated to the combination of *E/Z* configuration on the C=N double bond, bulk of the R group, and preferred conformations.[19] Metal coordination complexes and polymers have been obtained by using oximes as ligands.[20] 2-D coordination polymers have been obtained using 3-hydroxyiminomethyl salicylic acid;[21] Croitor et al.[22] obtained a variety of coordination networks through a mixed ligand approach, employing oximes with different coordination capacities and preferences. Gerasimchuk and co-workers have been exploring the potential of 2-cyanoximes as ligands in coordination polymers for a variety of applications.[23] Cai et al.[24] incorporated the oxime moiety as side group in oligo(ethylene glygol) monomethyl ether methacrylate (OEGMA) random copolymers, thus obtaining water-soluble polymethacrylates that switch their pre-organization and thermoresponsive behavior via light-tuned hydrogen bonding. Their work, which is possibly the first step towards exploiting the versatility of oxime residues in multi-functional polymers, recently stimulated us to copolymerize an HIA-containing methacrylate with OEGMA to obtain multi stimuli-responsive copolymers (Figure 1b).[1] Our first results elicit further insight into the dependence of some physico-chemical properties of HIAs on their structure. Specifically, the oxime Bond Dissociation Enthalpies (BDEs) and the structure and stability of the resulting >C=NO• radical may relate to reactions interfering with radical polymerizations, such as addition to the C=N bond or H abstraction. We also observed that the *E*/*Z* switch at photostationary state,[25] is very limited in the case of the polymer in Figure 1b and we surmise that it may be enhanced by inserting a different spacer between the HIA group and the polymer backbone. The rate of thermal reversal to the pre-photostimulation *E*/*Z* ratio and the occurrence of further photoinduced reactions may be also structure-dependent. Aiming at a rational design of an HIA-functionalized methacrylate for the synthesis of multi-stimuli responsive polymers, in the present investigation we explore the photochemical and physico-chemical properties of HIAs bearing substituents of different size and nature (Scheme 1). We focused on the R-group effect on oxime acidity and redox potential, UV-Vis spectra in solution, photochemical behavior with subsequent thermal relaxation, and Bond Dissociation Enthalpies.

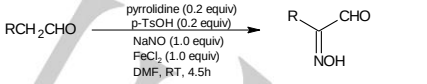

R	R
1: $CH_3(CH_2)_7$-	**9:** $CH_3(CH_2)_7$-, 59%
2: $[CH_3(CH_2)_9][CH_3(CH_2)_7]CH$-	**10:** $[CH_3(CH_2)_9][CH_3(CH_2)_7]CH$-, 60%
3: $(CH_3)_3C$-	**11:** $(CH_3)_3C$-, 65%
4: $CH=C(CH_3)CO_2(CH_2)_4$-	**12:** $CH=C(CH_3)CO_2(CH_2)_4$-, 60%
5: Cyclohexyl	**13:** Cyclohexyl, 93%
6: Ph-	**14:** Ph-, 90%
7: PhCH-	**15:** PhCH-, 67%
8: Np-	**16:** Np-, 45%

Scheme 1. Synthesis of 2-(hydroxyimino)aldehydes

Results and Discussion

Synthesis of HIAs

All HIAs were obtained by α-oximation of the precursor aldehydes according to a procedure developed in our laboratory (Scheme 1). The α-oximation reactions were performed at room temperature in dimethylformamide (DMF), with $NaNO_2$ and $FeCl_3$, in the presence of pyrrolidine as organocatalyst, resulting in satisfactory (45%) to excellent yields (90%).[5] Compounds **9**, **11**, **13**, **14** and **15** were obtained from their commercially available precursor aldehydes as already described in a previous report.[5] HIA **12** was obtained in good yields via a multi-step synthesis as we recently reported (Scheme 2).[1] Briefly, 1,6-hexanediol was monoacylated with methacrylic anhydride, and the resulting 6-hydroxyhexyl methacrylate **17** was oxidized to the corresponding aldehyde **4** through Parikh and Doering oxidation. α-Oximation of **4** gave, finally, 60% of product **12** after purification (Scheme 1). 3-Octyl-2-(hydroxyimino)tridecanal (**10**) and 2-(hydroxyimino)(naphthalene-2-yl)ethanal (**16**) and their precursor aldehydes **2** and **8** were first synthesized in this investigation. Scheme 3 outlines the synthesis of **2** and **8**. Specifically, 3-octyltridecanal **2** was prepared by Parikh and Doering oxidation[26] of 2-octyldodecanol **18** to aldehyde **19** in very good yield (90%). Wittig reaction of 2-octyldodecanal **19** with phosphonium ylide

$CH_3OCHPPh_3$ to enol ether **20** (yield 69%) and hydrolysis of this intermediate gave the 3-octyltridecanal **2** in excellent yield (94%).

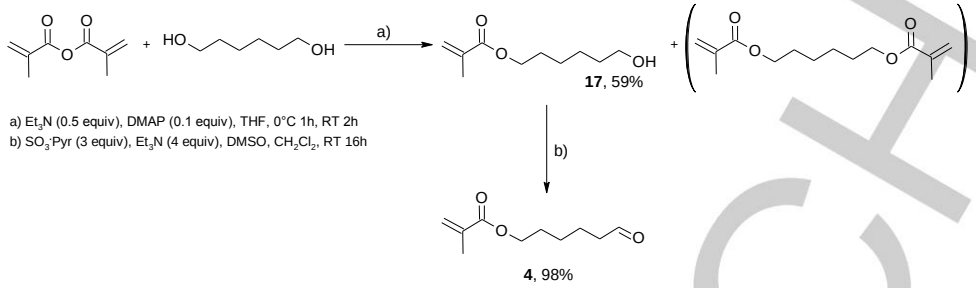

Scheme 2. Synthesis of HIABMA **4** (4-[(hydroxyimino)aldehyde]butyl methacrylate)[1]

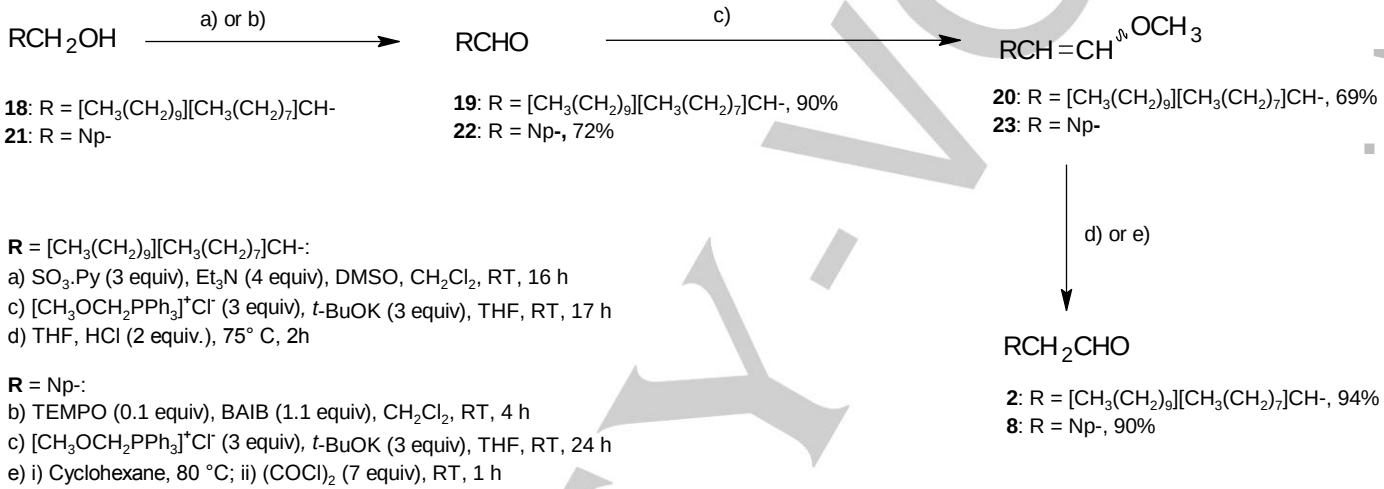

Scheme 3. Synthesis of 3-octyltridecanal **(2)** and 2-(naphthalen-1-yl)acetaldeyde **(8)**

Finally, compound **10** was obtained in fair yield (60%) by α-oximation of **2** (Scheme 1). As shown in Scheme 3, the oxidation of 1-naphthylmethanol **21** with 2,2,6,6-tetramethylpiperidine-1-oxyl radical (TEMPO) in the presence of the stoichiometric oxidant [bis(acetoxy)iodo]benzene (BAIB),[27] gave naphthalene-1-carbaldehyde **22** in good yield (72%). The next step was the Wittig reaction of aldehyde **22** with phosphonium ylide $CH_3OCHPPh_3$ to obtain the enol ether **23**.[28]
The crude product was extracted with cyclohexane, then thorough removal of phosphine oxide by-product was achieved by treatment with oxalyl chloride to obtain a mixture of compound **23** and aldehyde **8**.[28] Hydrolysis of this mixture in THF with concentrated hydrogen chloride[29] gave 1-naphthylacetaldehyde **8** in quantitative yield (90% vs aldehyde **22**) and high purity (GC: 95%). The final α-oximation reaction of **8** gave a reasonable (45%) yield of product **16** after purification.

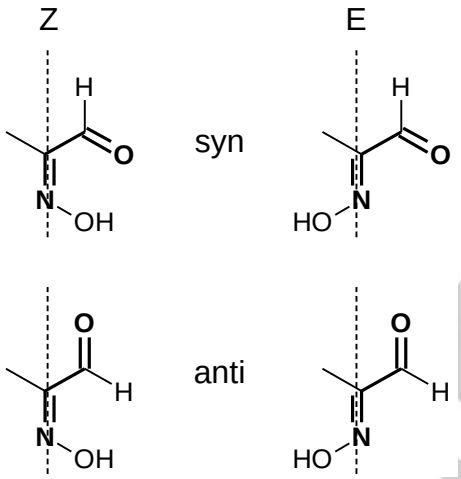

Figure 2. Configurational (*E*/*Z*) and conformational (*syn*/*anti*) isomers of 2-(hydroximino)aldehydes

Photochemical behavior of HIAs

Due to the presence of the C=N double bond, different configurational and geometrical isomers can be envisaged for HIAs (Figure 2). Oximes exhibit a complex photochemistry involving isomerizations, rearrangements, dehydration to nitriles or loss of the hydroxylamine function to form the parent carbonyl. The reader should refer to Roth's comprehensive review[30] to appreciate the richness of oximes photochemistry. Since it was first observed in 1890, *E*/*Z* photo- and thermal isomerism has been constantly an object of interest, with the first NMR studies in the late 1950s, all the way to recent computational studies on isomers interconversion.[31] Concerning the mechanism for *E*/*Z* isomerization, the transition state may be either linear, with the nitrogen atom turning its hybridization from sp^2 to sp, or a state where the imine double bond character is weakened, thus lowering the barrier for rotation about the C=N(OH) bond. Blanco et al.[32] attribute the former to ground state interconversion and the latter to photoinduced isomerization. From literature inspection,[30] it is quite clear that the propensity for photoisomerization, the relative stability of the configurational isomers and the complexity of the resulting mixtures are peculiar to the specific substituent adjacent to the oxime group. α-Oxo-oxime ethers were extensively investigated by Cerfontain and co-workers (see Ref.[33] and references therein), who showed that, in addition to *E*/*Z* interconversion, photolysis and/or a Norrish type II reaction can take place upon photoexcitation. The photoreactivity of α-oxo-oxime esters has been known for over a century and is still being investigated for the photoinitiation of acrylic monomers polymerizations.[34] In the present work, we carried out an NMR-based investigation on photo- and thermal isomerism of several HIAs. The investigated compounds differ by the bulk of the aliphatic R group (**9**: R= $CH_3(CH_2)_7$-; **10**: R= $[CH_3(CH_2)_9][CH_3(CH_2)_7]$CH-); **11**: R= $(CH_3)_3$CH-) or by the type of substituent (**12**: R= $CH_2=C(CH_3)CO_2(CH_2)_4$-; **14**: R= Ph). Compound **12** bears a remote methacrylate group, which is of interest for the synthesis of polymeric materials. In order to investigate the photoisomerization of HIAs, we carried out a preliminary study on their UV-visible absorption in several solvents. To follow the N-O*H* and C*H*O signals of the irradiated samples by ^{1}H-NMR analysis, we chose DMSO-d_6 (UV cutoff: 265 nm) for our photostimulation experiments. HIA solutions in DMSO-d_6 were then irradiated in a high pressure mercury lamp with an emission maximum at 350 nm. In a first set of experiments, the samples were photoexcited for a relatively short time, i.e. for up to 2h. No ^{1}H-NMR-detectable difference was observed between 1h and 2h irradiation, so we assume that a photostationary state had been reached. As detailed below, *E*/*Z* isomerization was observed within this timeframe. The samples were then allowed to thermally equilibrate at 40°C in the dark and were monitored by NMR over time. In a second set of experiments, photoexcitation was continued overnight (22h). In this case, significant, if not quantitative, formation of a single new product was observed. Based on the evidence presented in this paper and on the behavior of α-oxo-oximes documented by Buys et al.,[35] we identified this product as a cyclobutanol oxime (CBO) derivative (Scheme 4) from the Norrish-Yang cyclization.[36]

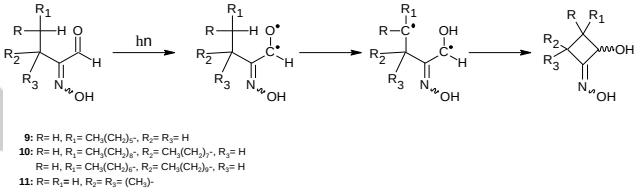

9: R= H, R_1= $CH_3(CH_2)_7$-, R_2= R_3= H
10: R= H, R_1= $CH_3(CH_2)_9$-, R_2= $CH_3(CH_2)_7$-, R_3= H
R= H, R_1= $CH_3(CH_2)_9$-, R_2= $CH_3(CH_2)_9$-, R_3= H
11: R= R_1= H, R_2= R_3= $(CH_3)_3$-

Scheme 4. Norrish-Yang cyclization of some HIAs.

UV-vis spectroscopy of HIAs

With the exception of the white or off-white solid HIAs **11**, **14** and **10**, all synthesized HIAs are colorless oils. The UV spectra at 0.1-0.5 mM concentration in several solvents are included in the Supporting Information (Table S1). A protic (*i*-PrOH) and three aprotic solvents of different polarity ($CHCl_3$, CH_3CN, DMF) were selected so as to ensure solubility of most of the HIAs under investigation and to highlight any band shifts caused by solvent effects. Consistently with literature on oximes and α-oxo-oximes,[30] all non-conjugated compounds show an allowed band at 230-240 nm (ε *ca.* 10000 $M^{-1}cm^{-1}$) ascribable to the π→π* transition. For HIAs **14** and **16**, having an aromatic ring as substituent on C(=NOH)CHO group, the same absorption band is shifted to *ca.* 270 nm. Spectra of concentrated (up to 1.2 mM) DMSO solutions of **10** and **12** were also recorded to check for the presence of a band ascribable to the forbidden *n*→π* transition.[36] Indeed, both **10** and **12** exhibit a weak band (ε <100 $M^{-1}cm^{-1}$) at 320-334 nm band, similarly to α-oxo-oximes.[30] Following deprotonation with $(CH_3)_4NOH$ as the base, a new peak appears at 290-300 nm due to the π→π* absorption bands of HIA anions, which delocalize the negative charge as depicted in Figure 3.[37] In contrast to amide-[38] and aryl-cyanoximates,[37a, 37b] the position of these bands in the spectra does not show a significance solvent dependence, the absorption maxima being in all cases around 290 nm.

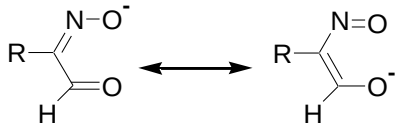

Figure 3. Negative charge delocalization of 2-(hydroxyimino)aldehyde anions

E/Z photo- and thermal isomerism

^{1}H-NMR signals of C=NO*H* and C*H*O are diagnostic for *E/Z* isomerism of HIAs. In Figure 4, the expansions of spectra encompassing all aldehyde and oxime signals are shown with their intensities. ^{1}H-NMR spectra of as-synthesized **9** and **12**, i.e. of the two compounds that bear a primary carbon next to the oxime group, only exhibit, respectively, one C*H*O peak (1H) at 9.39 and 9.40 ppm and one NO*H* peak (1H) at 12.89 and 12.92 ppm. After 2h light exposure of **9** or **12** in the photoreactor, two small additional peaks appear: 10.28 ppm (C*H*O) and about 12.00 ppm (NO*H*). The chemical shifts of the *aldehyde hydrogens* computed by DFT methods for the different isomers (Figure 2) of selected HIAs are reported in Table 1. The effect of DMSO was modeled using a continuum approach, i.e. by means of the Polarizable Continuum Model (PCM).[39] The computed chemical shift values for the (*Z*)-*syn* isomers are at most 0.4 ppm upfield of (*E*) isomers. Hence, it is not possible to assign any C*H*O aldehyde signals falling in the 9.1-9.7 ppm region of the spectrum to either configuration based on chemical shift calculations alone. However, the downfield NO*H* signal of unhindered α-oxo-oximes was assigned by Baas and Cerfontain [37c] to the *E*-anti isomer, the most stable due to dipolar interactions. On these grounds, we assume that signals around 12.9 ppm of unhindered HIAs **9** and **10** should be assigned to NO*H* in the *E* form. Hence, the signals around 9.4 ppm are attributed to the C*H*O of the *E* isomers. The calculated C*H*O chemical shifts for the (*E*)-*syn*/*anti* isomers (Table 1) are in good agreement with the experimental signals (Figure 4). However, since rapid interconversion (on the NMR timescale) of *E* conformers cannot be ruled out with such little hindrance to rotation of the CHO group, we are not assigning the (*E*)-**9** and (*E*)-**10** signals to either conformation. The calculated C*H*O shift for the (*Z*)-*anti* isomer (10.4 ppm) lies very close to one of the two signals (**b'**: 10.28 ppm) appearing after 2h irradiation. Since the intensity of the (*Z*)-NO*H* (12.00 ppm) signal matches that of (*Z*)-*anti* C*H*O, we surmise that only the (*Z*)-*anti* isomer is formed upon photostimulation. The pristine secondary compound **10** is also in the *E* form only (C*H*O peak at 9.34 ppm and NO*H* peak at 12.83 ppm). Upon photoexcitation, two small signals appear at 12.04 and 10.32 ppm, which we assign to the *Z* form in analogy with the primary compounds. The assignment of a further significantly intense signal at 10.15 ppm will be discussed later. As for tertiary **11**, similar arguments as for **9, 10** and **12** hold for the assignment of NMR signals to the *E* and *Z* isomers. However, in contrast with these compounds, the *Z* isomer (NO*H* and C*H*O signals of equal intensity at 11.78 and 10.24 ppm, respectively) is predominant over *E* (12.89 and 9.28 ppm of same intensity) prior to irradiation. In fact, (*E*)-**11** may be destabilized by overcrowding of the *t*-Bu group and N-OH group on the same side of the C=N bond. Photostimulation induces a complete switch in the configuration ratio and the appearance of a further signal at 10.14 ppm, which will be discussed later. In the case of compound **14**, the most relevant changes upon irradiation are detected in the aromatic region, whereas evidence for *E*/*Z* isomerization is too weak for any interpretation. Quantitative results for *E*/*Z* photoisomerization and subsequent thermal relaxation are summarized in Table 2. When HIAs bearing a primary R group (compounds **9** and **12**) are irradiated for two hours, limited inversion of configuration is observed (*E*/*Z*= 10/1). Thermal relaxation to *E*-isomer is quantitative in **9** within 8 days, while with HIA **12** the *E*/*Z* ratio is essentially unchanged after about three weeks. The remote methacrylate group, therefore, appears to slow down the thermal isomerization process. Also in the case of secondary **12** the *E* isomer is still predominant after 2h irradiation (*E*/*Z*~ 5/1) and thermal reversal to the *E* form is not completed after one week (*E*/*Z*~ 7/1). The most remarkable effect of 2h photostimulation is that observed with compound **11**. In fact, *E*/*Z* ratio switched from 1/10 to 5/1 and thermal relaxation was still incomplete after 40 days (*E*/*Z*= 1/2).

10.1002/chem.201800059

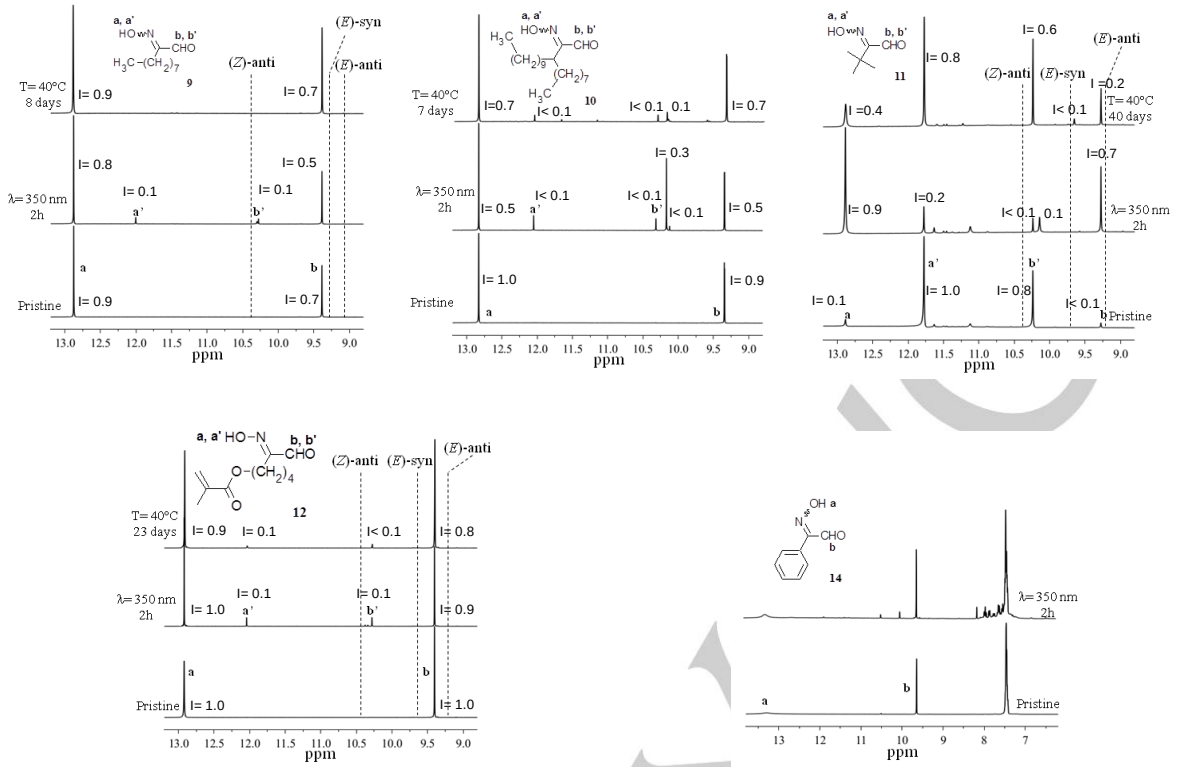

Figure 4. Expansion of the ^{1}H-NMR spectra (DMSO-d_6, δ : ppm) for the study of E/Z isomerism of compounds **9**, **10**, **11**, **12** and **14** after 2h photostimulation (λ = 350 nm) followed by annealing at 40°C. Intensities are normalized to terminal –C*H*$_3$ (**9**, **10**, **11**) or -OC*H*$_2$- (**12**). Broken lines are a pictorial of the calculated chemical shifts (Table 1) for different geometrical and conformational isomers of HIAs. Full spectra in the Supporting Information.

Table 1. ^{1}H-NMR computed chemical shifts[a] for the C*H*O of the different configurational and conformational isomers of HIAs.

RC(NOH)CHO	(*Z*)-*anti* (δ)	(*Z*)-*syn* (δ)	(*E*)-*anti* (δ)	(*E*)-*syn* (δ)
(9) $CH_3(CH_2)_7$-	10.4	9.1	9.1	9.3
(11) $(CH_3)_3C$-	10.4	9.3	9.2	9.7
(12) $CH_2=C(CH_3)CO_2(CH_2)_4$-	10.4	9.2	9.2	9.6

[a]Geometry optimization in vacuum at the B3LYP/6-31+G(d, p) level; Chemical shift calculations with WPO4/aug-cc-pVdZ; effect of the solvent modeled by means of the PCM. δ : ppm.

Table 2 *E*/*Z* photoisomerization[a] and thermal re-equilibration[b] of selected HIAs.

RC(NOH)CHO	Time	*E*/*Z*
(9) $CH_3(CH_2)_7$-	t=0	*E* only
	2h, 350 nm[a]	10/1
	8 days, 40°C[b]	*E* only
(10) $[CH_3(CH_2)_9][CH_3(CH_2)_7]CH$-	t=0	*E* only
	2h, 350 nm[a]	~5/1
	7 days, 40°C [b]	~7/1
(11) $(CH_3)_3C$-	t=0	1/10
	2h, 350 nm[a]	5/1
	40 days, 40°C [b]	1/2
(12) $CH_2=C(CH_3)CO_2(CH_2)_4$-	t=0	*E* only
	2h, 350 nm[a]	10/1
	23 days, 40°C [b]	10/1

[a] Irradiation (λ = 350 nm) in DMSO-d_6 followed by ^{1}H-NMR analysis.
[b] After irradiation, the samples were stored in the dark at 40°C and analyzed by ^{1}H-NMR at suitable time intervals.

Photoisomerization to cyclobutanol oxime (CBO)

As anticipated in the previous paragraph, compounds **10** and **11** exhibit additional ^{1}H-NMR peaks (10.15 and 10.14 ppm, respectively) besides those ascribed to *E*/*Z* isomerization, already within 2h of photostimulation. Indeed, halving of the *E*-isomer CHO and NOH peak intensities to the benefit of one single signal at 10.15 ppm is the most prominent effect of the 2h irradiation of compound **10** (Figure 4). In order to better observe any photoreactions that may occur over longer timescales than *E*/*Z* interconversion, photostimulation of compounds **9**, **11** and **10** was continued overnight (22h). Some features can be observed in the ^{1}H-NMR spectra of the resulting solutions (Supporting Information S14-S22; Figure 5):

i) (*Z*)-*anti* signals are negligible; (*E*)-isomers signals are still present;

ii) The main photoproduct formed exhibits a singlet at 10.1-10.2 ppm (1H) and a set of signals in the 5.5 (1H) and 4-5 ppm (1H) regions of the spectra. D_2O exchange shows that protons at 5.5 ppm exchange rapidly and couple with the 4-5 ppm protons (see Supporting Information S15);

iii) A signal at 8.13 ppm peak is observed independently of the HIA substituent. This signal can be attributed to formic acid, i.e. the by-product formed by decomposition of HIAs to nitriles.[30]

In order to identify the product originating the new set (see feature *ii* above) of ^{1}H-NMR signals, we focused on **10**, which shows the least amount of residual HIA and of minor decomposition products. Full ^{1}H- and ^{13}C- NMR spectra of **10** after 22h irradiation, shown in Figure 5, are compatible with the formation of a cyclobutanol oxime (CBO) from Norrish-Yang cyclization,[36] as depicted in Scheme 4.

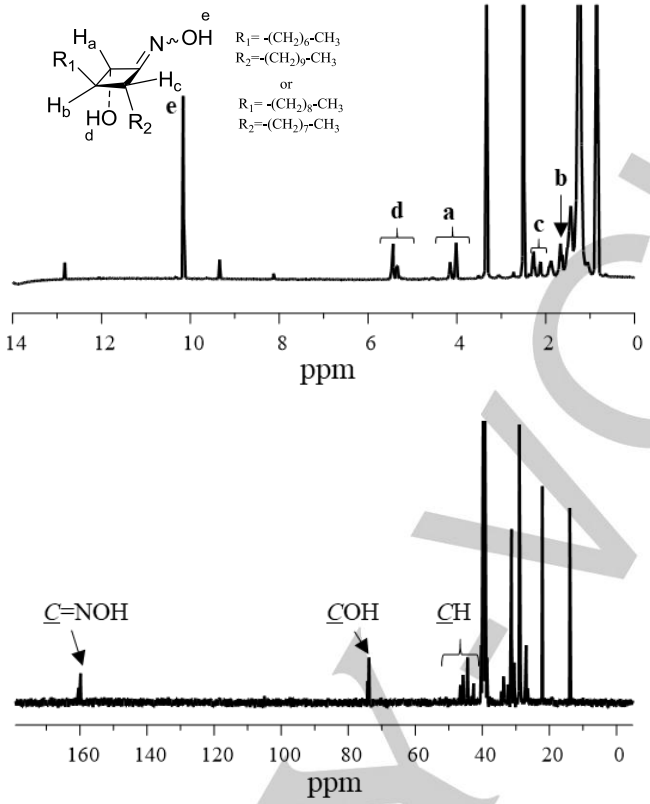

Figure 5. ^{1}H-NMR and ^{13}C-NMR (DMSO-d_6) spectra of **10** after 22h photostimulation (λ= 350 nm) followed by 4h at room temperature. δ (ppm): 12.8 (HIA, C=NO*H*, 0.1); 10.2 (H_e, 1.2); 9.34 (HIA, C*H*O, 0.1); 5.45 and 5.35 (H_d, 0.6 and 0.3); 4.15 and 4.02 (H_a, 0.3 and 0.7); 2.27 and 2.12 (H_c, 0.7 and 0.3); 1.65 (H_b, 1.0).

Unequivocal evidence is provided by D_2O exchange and 2D NMR experiments (Supporting Information S15-S20). Specifically, the ^{1}H-NMR spectrum is simplified upon the addition of D_2O due to the disappearance of two exchangeable protons (10.15 ppm and 5.45 ppm). These signals can be attributed, respectively, to the C=NO*H* and CH-O*H* protons of the CBO structure. Further NMR experiments (COSY, DEPT 135, NOESY, HSQC; Supporting Information S15-S20) contribute to the assignment of the C*H* ring signals (reported in Figure 5), whereas the HMBC experiment clearly confirms the cyclic structure. In fact, the oxime carbon (159.8 ppm) shows long-range correlation with C-H_a and C-H_c , while C-H_b has $^{2}J_{CH}$ with the alcoholic carbon (74.3 ppm). It is worth noting that the formation of the cyclobutanol ring (Scheme 4) requires the HIA to be in the *anti* conformation, regardless of geometrical isomerism.[40] Upon thermal annealing, occurring even as the NMR spectra are acquired at room temperature, *E*/*Z* equilibration of the oxime group in the CBO structure takes place, as shown by the more complex NMR spectrum (Figure 5) with different C*H*-O*H* signals and splitting of its oxime signal (Supporting Information S15, inset). When compound **9** is irradiated for 22 h (Supporting Information S14), the HIA oxime and aldehyde (*E* isomer, 12.89 and 9.39 ppm) signals are only partially reduced and signals at 10.3 ppm, 5.64 and 5.46 ppm, 4.21 and 4.72 ppm are present, which are consistent with the formation of both *E* and *Z* isomers of CBO. 22h irradiation of compound **11** also yields the CBO structure (Supporting Information S21; 10.15, 5.50, 4.61 ppm) along with residual HIA**.** However, a number of unidentified minor signals are also detected. Table 3 shows the quantitative outcome of *E*/*Z* and Norrish-Yang photoisomerization of **9**, **10** and **11**.

Table 3 *E*/*Z* vs. Norrish-Yang photoisomerization of selected HIAs.[a]

RC(NOH)CHO	Time	HIA *E*/*Z*	CBO/HIA[b] (CBO%)
(9) $CH_3(CH_2)_7$-	t=0	*E* only	nd[c]
	2h, 350 nm	10/1	<1%
	22h, 350 nm	*E* only	0.7/1 (40%)
(10) $[CH_3(CH_2)_9][CH_3(CH_2)_7]CH$-	t=0	*E* only	nd[b]
	2h, 350 nm	~5/1	0.5/1 (30%)
	22h, 350 nm	*E* only	20/1 (95%)
(11) $(CH_3)_3C$-	t=0	1/10	nd[b]
	2h, 350 nm	5/1	0.1/1 (9%)
	22h, 350 nm	6/1	12/1 (77%)

[a] Irradiation (λ = 350 nm) in DMSO-d_6 followed by ^{1}H-NMR analysis.

[b] Intensity of NO*H* signal of CBO/total C*H*O signal (both *E* and *Z*); CBO% = 100xCBO/(CBO+HIA).

[c] No CBO detected by NMR.

The *Z* isomers of **9** and **10** are only observed upon short time irradiation (*E*/*Z* 10/1 and 5/1, respectively) and are no longer detected after 22h exposure to light. After 22h, **10**- and **11**-CBO formation is almost quantitative (95 and 77%, respectively) and less remarkable in **9** (40%). It should be noted that **i**n these experimental conditions configuration inversion of HIA **10** appears to be associated with sizable amounts of CBO at all irradiation times. In the case of **11**, instead, it is possible to obtain inversion of configuration after 2h photostimulation with less than 10% CBO formation.

Electrochemical properties, acidity and O-H bond dissociation enthalpies of HIAs

As outlined in the introduction, oximate ions find important applications related to their nucleophilic properties and to their ability to form metal complexes. Particularly, oximate ions of low basicity (pK_a< 9) exhibit an enhanced nucleophilicity relative to alkoxide anions, due to the α-nucleophile effect. This property, which has drawn considerable attention towards oximes in the detoxification of organophosphorous compounds, levels off as the acidity of the parent oxime decreases.[11] The capacity of oximes and their anions to form metal coordination complexes can be used in multiple-analyte and/or electrochemical systems for detection of metal ions or other organic species.[41] Redox properties and acidity of oximes are important properties to assess in view of these applications. In the case of HIAs, the presence of the electron-withdrawing CHO substituent on the C(=NOH) group is expected to enhance their acidity and affect the oxidation potential of their anion with respect to the corresponding unsubstituted oxime/oximate pairs. A further property of HIAs that is worth investigating is their Bond Dissociation Enthalpy (BDE). The energy involved in the homolytic dissociation of the NO-H is an important factor in the metabolic activity of oximes (Ref.[42] and references therein) and in evaluating the H-abstraction by other radical species that may be present in a reaction environment, to yield α-CHO iminoxyl radicals. For instance, in our previous investigation on the RAFT copolymerization of an HIA-containing methacrylate,[1] we were left with the question of HIAs undergoing H-abstraction as a possible interfering reaction. Potential H- acceptors are the 2-cyanopropyl radicals resulting from the decomposition of the AIBN initiator or of the 2-cyanoprop-2-yl(4-fluoro)dithiobenzoate chain-transfer agent, as well as the carbon-centered radicals in the propagating polymer chains. In fact, literature values for the BDE of 2-methylpropanenitrile are reported in the 85-92 kcal mol^{-1} range, and those of unconjugated C-H bonds are likely to approach 100 kcal mol^{-1}.[43] BDEs of simple oximes, instead, usually fall in the 77-90 kcal mol^{-1} range.[42, 44] However a plain comparison of gas-phase BDEs, which do not take into account solvent effects, is not conclusive proof of the formation of >C=NO• species in the polymerization conditions. Anyway, assessing the relationship between BDEs and HIA structures is a starting point in investigating some aspets of the radical polymerization of HIA-functionalized monomers.

As we are not aware of any previous investigation on the pK_a, and oxidation potential of HIAs, we have determined their values for the compounds included in the present work. As regards the BDEs, we compared the calculated gas-phase O-H bond dissociation enthalpies of tertiary **11** and HIA-functionalized methacrylate **12**. The latter also serves as a model compound for HIAs bearing a linear R substituent.

Determination of oxidation potentials

HIA oxidation potentials were determined by cyclic voltammetry. Measurements were carried out at a scan rate of 0.5V/sec in DMF, using 0.1M Bu_4NBF_4 as the supporting electrolyte, a glassy carbon working electrode and an Ag/AgCl/KCl 3M reference electrode. Figure 6 shows representative voltammograms of **10**, **12** and their anions. All other traces are reported in the SI. Potentials were first swept to 2V/NHE. Similarly to simple ketoximes and aldoximes,[37c, 38] none of the HIAs were oxidized even at this potential. After deprotonation with a 4-fold excess of Me_4NOH, all 2-(hydroxyimino)aldehyde anions show two irreversible oxidation peaks (Table 24, Figure 6 and SI), the first in the 0.40 - 0.65 V/NHE range, the second at E>1.1V/NHE. The latter is more pronounced in **10**$^-$, **11**$^-$, **13**$^-$. When the potential was switched at 0.8V/NHE (scan rate of 0.5 V/s), oxidation peak of **10**$^-$ (E^p = 0.52V/NHE) and **15**$^-$ (E^p = 0.61V/NHE)

remained irreversible, while that of **12**$^-$ (E^p = 0.64V/NHE) and all other anions became partially reversible (Figure 6, insets). A more detailed investigation on the chemical processes causing this lack of reversibility is currently in progress. Anyway, these results indicate that 2-(hydroxyimino)aldehyde anions, with the exception of compound **11**$^-$ having a bulky substituent (E^p = 0.38V), are oxidized at higher potentials than simple aldoximes (CH_3CH=NOH, E^p= 0.137V/NHE; (E)-PhCH=NOH, E^p= 0.328V/NHE) and ketoximes ($(CH_3)_2C$=NOH E^p= 0.181 V/NHE; Ph_2C=NOH, E^p= 0.225V/NHE).[40-41] Indeed, oxidation potentials of HIA anions are more similar to those of α-ketoximes (CH_3COCH=NO^-, E^p= 0.558V/NHE; PhCOCH=NO^-, E^p= 0.540 V/NHE)[45] bearing a carbonyl group in conjugation to the >C=NO^- moiety.

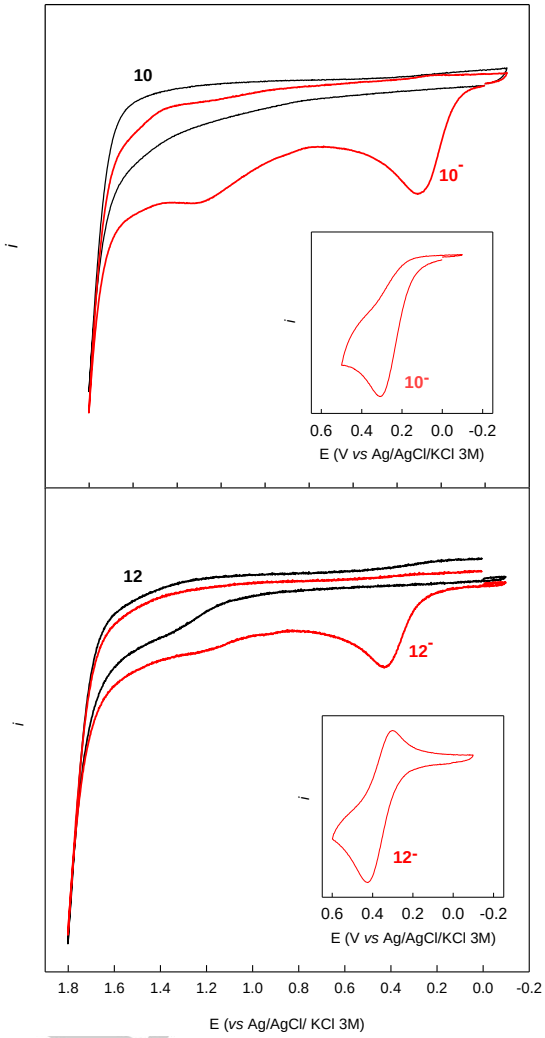

Figure 6. Cyclic voltammetry of 2-(hydroxyimino)aldehydes **10**, **12** and their anions in DMF at 0.5 V/s

Determination of pK_a

The pK_a of HIAs **9-16** was determined by potentiometric titration. Due to their insolubility in pure water, all HIAs except **10** were dissolved in DMSO/water mixtures (10/90, 20/80 and 30/70, v/v) and titrated with KOH 0.1 M in the presence of KCl (0.15 M) to maintain a constant ionic strength. For each DMSO/water mixture, experiments were carried out at least twice and the corresponding p$_s$K$_a$s were calculated using Henderson-Hasselbalch equation. Aqueous pK_a values were then derived from p$_s$K$_a$ data through the Yasuda-Shedlovsky equation (Table 4).[42]

Table 4. pK_a of 2-(hydroxyimino)aldehydes and oxidation potential (E^p) of the corresponding anions

RC(NOH)CHO	pK_a[a]	E^p (V *vs.* NHE)[b]
(**9**) $CH_3(CH_2)_7$-	8.8 ± 0.2	0.55 ± 0.01

(**10**) $[CH_3(CH_2)_9][CH_3(CH_2)_7]CH$-	8.7 ± 0.2[c]	0.52 ± 0.02
(**11**) $(CH_3)_3C$-	9.90 ± 0.03	0.38 ± 0.01
(**12**) $CH_2=C(CH_3)CO_2(CH_2)_4$-	7.68 ± 0.07	0.64 ± 0.02
(**13**) Cyclohexyl-	8.7 ± 0.3	0.51 ± 0.01
(**14**) Ph-	7.69 ± 0.02	0.63 ± 0.01
(**15**) $PhCH_2$-	8.05 ± 0.07	0.61 ± 0.01
(**16**) Np-	7.94 ± 0.06	0.60 ± 0.02

[a] In pK_a units; p_sK_a were determined by potentiometric titration in DMSO/mixtures and converted to aqueous pK_a by the Yasuda-Shedlovsky equation:[46] $p_sK_a + \log[H_2O] = a + b/\varepsilon$
[b] Oxidation potential were determined by CV in DMF at scan rate 0.5 V/s, using a glass carbon working electrode and Ag/AgCl/KCl 3M reference electrode; oxidation potential are referred to NHE by equation: E(V vs. NHE) = E(V vs. Ag/AgCl/KCl 3M) + 0.21[45]
[c] Determined by linear regression of plot pK_a *versus* E^p (see text)

Unfortunately, HIA **10** was not soluble in any DMSO/water proportion. Based on values in Table 4, however, we are able to show a correlation of pK_a and E^p values. A plot of pK_a of HIAs *vs.* the E^p of the corresponding anionsis, indeed, fairly linear (Figure 7) and, from linear regression of all data (r^2= 0.96), it has been possible to estimate for compound **10** a pK_a of 8.7.

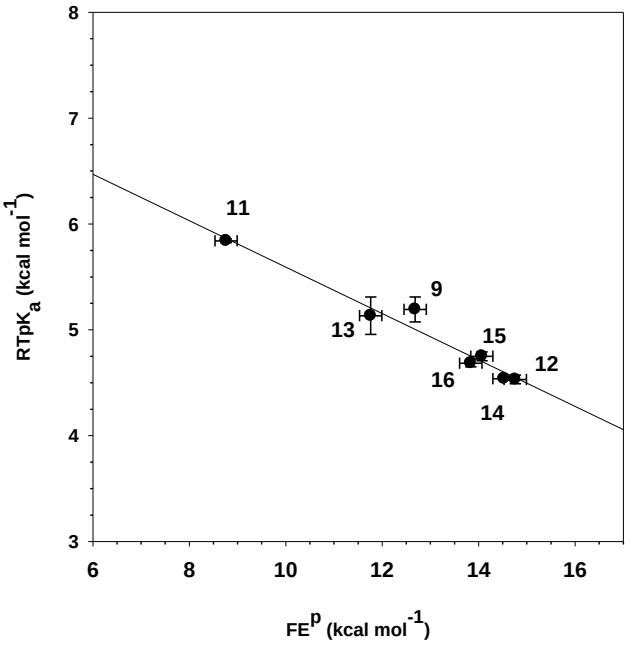

Figure 7. Plot of pK_a of 2-(hydroxyimino)aldehydes *versus* oxidation potential of the corresponding anions

As shown in Table 4, the values of measured pK_a for all HIAs fall within a narrow range (2.2 pK_a units) around 7.7-9.9, so they are weaker acids than α-arylcyanoximes (pK_a range 4.5-6.2).[35] Their acidity is, instead, comparable to that of hydroxamic acids, ranging approximately from 7.9 for $C_6H_5C(O)N(OH)CH_3$[45] to 9.9 for $(CH_3)_3C(O)N(OH)CH_3$.[46] As highlighted by the linear correlation in Figure 7, compound **11**, i.e. the HIA bearing the bulkiest R group, is the least acidic among the investigated HIAs and its anion shows the lowest oxidation potential. These properties could be related to poorer solvation of the anion, or to the steric effect of the *t*-Bu group.

Table 5. Calculated bond lenghts (Å) and angles (degrees) for HIAs 11 and 12 with their corresponding anions and radicals in DMF[a]

RC(NOH)CHO	r(R-CN)	r(C-CO)	r(C=N)	r(N-O)	r(C=O)	∠RCN	∠RCC	∠CCN	∠CNO
(*Z*)-**11** *syn/anti*	1.53/1.53	1.48/1.50	1.29/1.28	1.37/1.39	1.23/1.21	118.35/117.37	118.66/121.64	123.00/120.99	119.17/115.22
(*Z*)-**11** *syn/anti*	1.54/1.53	1.44/1.44	1.33/1.34	1.29/1.30	1.24/1.24	116.84/117.68	117.15/121.98	126.00/120.34	120.51/120.50
(*Z*)-**11**$^{\bullet}$ *syn/anti*	1.52/1.52	1.48/1.48	1.29/1.29	1.22/1.22	1.21/1.21	120.89/120.33	122.41/124.70	116.71/114.95	132.55/135.02
(*E*)-**12** *syn/anti*	1.50/1.50	1.50/1.48	1.28/1.29	1.38/1.38	1.21/1.21	126.28/127.04	118.63/121.23	115.09/111.73	112.86/113.18
(*E*)-**12** *syn/anti*	1.51/1.50	1.44/1.43	1.33/1.33	1.29/1.29	1.24/1.24	123.02/124.17	119.58/122.45	117.40/113.38	117.55/117.98
(*E*)-**12**$^{\bullet}$ *syn/anti*	1.51/1.50	1.48/1.47	1.29/1.30	1.21/1.22	1.21/1.22	121.52/122.41	122.40/123.52	116.07/114.07	133.73/133.94

[a] Geometry optimization at the B3LYP/6-311+G(2d,2p) level; effect of DMF solvent by means of the PCM

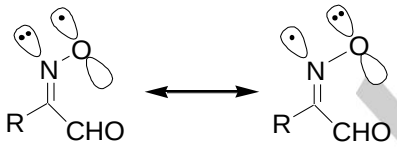

Figure 8. HIA radicals. Unpaired electron is localized on the N-O residue and lies in the CNO plane.

Indeed, as reported in the literature,[42, 44a] the O-H bond dissociation enthalpy of (t-Bu)$_2$C=NOH is about 5 kcal/mol lower than that of linear oximes. This effect has been ascribed to the smaller repulsion between the two *t*-Bu groups, and between *t*-Bu and O, in the iminoxyl radical than in the parent oxime. Similarly, one could expect a larger steric relief upon oxidation of **11**$^{-}$ to the corresponding adical than in the case of a linear, less hindered HIA^{-}.

In order to assess the role of steric relief in lowering both the acidity of **11** and the energy requirement for the oxidation of its anion, we computed the lowest-energy structures of **11**, **12** and of their corresponding anions and radicals by QM calculations. The effect of DMF, the solvent used for oxidation potential determinations, was modeled using the Polarizable Continuum Model (PCM). Since ^{1}H-NMR and computational analysis show that compound **11** exists mainly as isomer (*Z*)-anti (*Z*/*E* ≈10) while **12** is present exclusively as isomer *E* (see previous section), calculations were limited to the (*Z*)-**11** and (*E*)-**12** isomers, both in syn and anti conformations (Figure 2), with their corresponding anions and radicals. Discussion is focused on anti-(*Z*)-**11** and syn/anti-(*E*)-**12**. Results in Table 5 highlight some interesting structural features of HIA anions and radicals, regardless of substituent bulk. In anti-(*Z*)-**11** the C-CO and N-O bonds are shorter in the anion, compared to the parent compound (1.50 to 1.44 Å and 1.39 to 1.30 Å, respectively). Consistently, C=N and C=O bonds are lengthened (1.28 to 1.34 Å and 1.21 to 1.24 Å, respectively). Similar observations can be made for the **12**/**12** pair. Furthermore, the C(=NOH) and CHO groups in the optimized HIA/HIA structures are coplanar in both the syn and anti isomers. These results suggest that the structure of HIA anions can be described as intermediate between the two resonance forms depicted in Figure 2. It is worth noting that neither **11**, nor **12** exhibit any significant differences with their anions in terms of bond angles. Moreover, their values are quite similar when comparing the two HIA/HIA pairs. In contrast with the anions, HIA radicals exhibit very similar bond lengths as their parent compounds with the exception of the N-O bond, which is shorter by 0.15-0.17 Å, while ∠CNO angles increase by 13-20° for both **11** and **12**. For the radical species, the calculation of spin densities, performed at the UB3LYP/6-311+G(2d,2p) level, indicates a spin density of about 0.52-0.55 on O and about 0.43-0.47 on N atoms of the C(=NOH) moiety, while the oxygen of CHO group and all carbons have almost null values of spin densitiy. In agreement with previous literature on oximes,[42, 44a] these results suggest that the iminoxyl radical is of the σ type, i.e. the unpaired electron lies in the same plane as the local molecular framework (Figure 8). In other words, in contrast with the negative charge of the corresponding anions, the unpaired electron is not delocalized on the CHO substituent. Direct comparison of **11**$^{\bullet}$ and **12**$^{\bullet}$ with their respective anions shows that ∠CCN angles expand slightly more in the **11**$^{\bullet}$**/11** than the **12**$^{\bullet}$**/12** pair. The magnitude of these **11** *vs*. **12** differences, however, does not account for a significant steric effect in the radical relative to the anion forms of **11**.[44a] When all the above results are taken into account, it appears that the presence of the bulky *t*-Bu group on **11** affects both its acidity and oxidation potential through poorer solvation of the anion, rather than through a distortion of the anion or of the radical. This (lack of) solvation effect is expected to be particularly sizable in solvents such as water or DMF, which are able to form hydrogen bonds with the C(=NOH) and CHO groups.

Calculation of O-H Bond Dissociation Enthalpies of some HIAs

The calculated BDEs of **11** and **12** are reported in Table 6 along with literature BDE values of some symmetric ketoximes bearing alkyl substituents of different bulk.[44a] Firstly, results in Table 6 indicate that BDE values of HIAs are somewhat smaller than those of simple oximes. Substituting the CHO group for one of the ketoxime alkyl substituents to form the HIA lowers the BDE by about 3-10 kcal mol^{-1}. As reported in the literature, BDEs in ketoximes depend on geometrical isomerism, steric effects, dipole-dipole interactions and intramolecular hydrogen bonding. For instance, the BDEs of *E*-oximes are about 3-5 kcal mol^{-1} higher than those of the corresponding *Z*-isomers.[42, 44a] Indeed, this also applies to HIA **12**, even though the difference is limited to only 3 kcal mol^{-1}. Interestingly, the hindered HIA **11** exhibits an opposite trend (Table 6).

more destabilized less destabilized

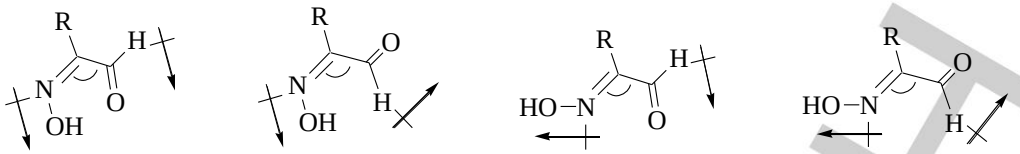

	∠CCN angles			
	Z-syn	***Z-anti***	***E-syn***	***E-anti***
11	122.9°	121.3°	110.7°	106.7°
12	123.3°	123.7°	115.4°	112.2°

Figure 9. Dipolar repulsions in the different isomers of HIAs. **11** and **12**. ∠CCN angles of from optimized geometries in the gas-phase at the B3LYP/6-311+G(2d,2p) level.

Table 6. Gas-phase O-H BDEs of 2-(hydroxyimino)aldehydes[a] at 298 K in kcal mol^{-1}

RC(=NOH)CHO	***Z-syn***	***Z-anti***	***E-syn***	***E-anti***
(**11**) $(CH_3)_3C$-	74.8	72.7	72.9	72.5
(**12**) $CH_2=C(CH_3)CO_2(CH_2)_4$-	75.5	74.4	75.7	77.5
t-$Bu_2C(N=OH)$		75.6[b]		
i-$Pr_2C(N=OH)$		80.7[b]		
$Et_2C(N=OH)$		81.8[b]		
$Me_2C(N=OH)$		82.6[b]		

[a] Calculated by DFT at the B3LYP/6-311+G(2d,2p) level of theory. [b] From Ref.[44a]

A small effect of the *syn*/*anti* isomerism is also observed, in that the BDEs of (*Z*)-*syn* isomers (both **11** and **12**) are about 2 kcal mol^{-1} larger than those of the corresponding (*Z*)-*anti* forms. Intramolecular hydrogen bond between the oxygen atom in CHO and the hydrogen in C(N=OH) is likely to be accountable for this energy difference. The O-H--O distances in the optimized geometries of *syn*-(*Z*)-**11** and *syn*-(*Z*)-**12**, indeed, are 2.57 Å and 2.60 Å in **11** and **12**, respectively, which is also indicative of hydrogen bonding. In agreement with the NMR results discussed in the previous section, our calculations in the gas phase confirm the greater stability (5-7 kcal mol^{-1}) of *anti*-(*E*)-**12** relative to all other isomers of **12** and the lesser stability (about 1-5 kcal mol^{-1}) of (*E*)-**11** relative to (*Z*)-**11**. We believe that this difference should be attributed to the combined effect of *t*-Bu bulk and dipole moments interactions, as explained next. In Figure 9 the calculated ∠CCN angles are reported for all isomers, together with a pictorial of the dipole moments associated with the C(N=OH) and CHO groups. While ∠CCN angles in *syn/anti*-(*Z*)-**11** and **12** are quite similar, the C(N=OH) and CHO groups (and the dipole moments associated with them) in *E* are brought closer together by the bulk of the *t*-Bu in **11** (∠CCN 107-111°) than by the less bulky substituent in **12** (∠CCN 112-115°). Dipolar interactions would therefore be more destabilizing in (*E*)-**11** than in **(***E*)-**12**. As for the gas-phase optimized structures of iminoxyl radicals, results are analogous to those obtained in DMF, in that the unpaired electron is of the σ-type, lying in the molecular framework plane. In all radicals, moreover, ∠CNO angles are in the 132-134°, i.e. larger than in the parent HIAs (∠CNO range: 112-119°), thus making dipole-dipole interactions less significant. The larger dipolar destabilization of HIA **11** relative to **12** and the corresponding larger relief in the radical optimized structures could rationalize the BDEs in (*Z*)-**11** and (*Z*)-**12** and the smaller BDEs of (*E*)-**11** with respect to (*E*)-**12** (Table 6).

Conclusions

We have presented a comprehensive investigation of the photochemistry and physico-chemical properties of a new class of organic compounds, 2-(hydroxyimino)aldehydes. The interpretation of experimental NMR, acidity and redox properties is corroborated by DFT calculations. UV irradiation (λ= 350 nm) results in two main phenomena, i.e. *E*/*Z* photoisomerization, occurring within two hours, and the slower, irreversible formation of cyclobutanol oxime (CBO) derivatives by a Norrish-Yang cyclization. To our knowledge, this is the first time that CBOs are described in the literature. The predominant initial configuration, the extent of light-induced isomerization and the rate of subsequent thermal annealing to the initial *E*/*Z* population are strongly dependent on HIA substituent. HIAs bearing primary and secondary substituents yield limited configurational inversion, whereas the presence of a tertiary group results in *E*/*Z* switch. Thermal relaxation in the dark to the initial configuration proceeds over weeks when HIA substituents are secondary or tertiary and is complete within days with a linear alkyl group. However, our results with a primary substituent bearing a remote methacrylate show that branching next to the HIA is not the only factor affecting the rate of thermal relaxation. Cyclization to CBO begins at the same time as *E*/*Z* isomerization and becomes predominant over long irradiation times. However, it is possible to obtain *E*/*Z* inversion with little CBO formation over short irradiation times of an HIA bearing a tertiary substituent.

As expected, the vicinity of the CHO and oxime groups causes the acidity of the latter to be stronger than that of simple oximes and close to that of hydroxamic acids. The oxidation potentials (E^p) of HIA anions are in line with those of α-oxo-oximes, i.e. higher than simple oximes. BDEs of the O-H bond of C(=NOH) group, calculated by DFT methods in vacuum, are lower than in simple oximes. BDEs of all isomers of a primary and a tertiary HIA are interpreted through differences in dipole-dipole interactions, which are found to be affected, in some isomers, by the bulk of the tertiary substituent.

This study confirms that the strong dependence of HIA photochemistry on the bulk and nature of substituents is of great interest towards designing different HIA-functionalized monomers. In fact, it should be possible to obtain polymers with opposite *E*/*Z* abundance, both at thermal- and photoequilibrium, and to exploit the differences in hydrogen bond-driven pre-organization in solution between the two configurations.[24] Furthermore, the photoisomerization of some HIAs to the CBO structure would constitute a strong response to UV light.

Experimental Section

Please refer to Supporting Information for details on chemicals, general instrumentation and yields and characterization of specific compounds.

HIA syntheses. General procedure

HIAs were prepared according to a procedure optimized in our laboratory.[5] Generally, under argon atmosphere, pyrrolidine (0.4 mmol, 33 µL) is added to a solution of p-TsOH monohydrate (0.4 mmol, 76 mg) in 3 mL of anhydrous DMF, followed by addition of distilled water (4.0 mmol, 72 µL) and aldehyde (2.0 mmol). After stirring for 5 minutes, $NaNO_2$ (2.0 mmol, 0.14 g) is added and then anhydrous $FeCl_3$ (2.0 mmol, 0.32 g) is carefully introduced in aliquotes to avoid overheating (use caution: exothermic reaction). Magnetic stirring is continued at room temperature and reaction progress is monitored by thin layer chromatography and GC or GC-MS analysis. Note that in gaschromatographic analyses, HIAs exhibit a slight decomposition to the corresponding nitrile derivatives as confirmed by comparison with authentic samples available in our laboratory. When no further reaction progress is observed (4.5 – 5.5 h), 5 mL of saturated NaCl solution is added and, after stirring for 30 minutes, the mixture is extracted with ethyl acetate (4x15 mL). The organic phase is washed with a saturated solution of NaCl and dried over Na_2SO_4. After evaporation of the solvent under reduced pressure, all products are purified by silica gel chromatography using a hexane/ethyl acetate gradient and characterized by spectroscopic analysis.

DFT calculations

The coordinates of the molecules were prepared using Molden software and all the calculations were performed with Gaussian 09 program.[47] For the calculation of the BDE the geometries of the neutral species and of the corresponding radicals were optimized by means of DFT using the B3LYP functional, the 6-311+G(2d,2p) basis set. The enthalpy correction terms have been estimated from the Hessian matrix.

To compare the effect of the substituents, the molecular geometries (here including also the corresponding anions) have been optimized using the same level of theory and including the solvent effect by means of the Polarizable Continuum Model (solvent DMF).

Concerning the NMR parameter estimates, the chemical shifts were computed using the procedure found in Pierens,[39] which provides the best estimate of the experimental values of the chemical shifts;[48] that is, the optimizations were performed in vacuo and

the shielding tensors were calculated by means of the PCM (solvent DMSO) using the WPO4 functional and the aug-cc-pVdZ basis set.
In all the optimizations described above, the computation of the Hessian matrix excluded the presence of negative frequencies.

Conflicts of interest

The authors declare no conflict of interest

Keywords: 2-(hydroxyimino)aldehydes • photoisomerism • acidity • bond energy • multi-stimuli responsive polymers

Note: § Bordwell et al.[49] measured irreversible oxidation potentials in DMSO (0.1 M Et_4NBF_4) by CV using a platinum working electrode and Ep values are reported vs. ferrocinium/ferrocene couple. To compare with our results, these potential values are referred to NHE electrode according to equation E(V vs.NHE) = E (V vs. Fc^+/Fc) + 0.75.

10.1002/chem.201800059

WILEY-VCH

Entry for the Table of Contents

FULL PAPER **2-(hydroxyimino)aldehydes**

Versatile oxime derivatives.
Photochemical and physico-chemical properties of a series of 2-(hydroxyimino)aldehydes (HIAs) were explored as a function of structural variations. Results show that HIAs are highly versatile molecules for many applications and that carefully-designed HIA-containing monomers should impart sensitivity to light, pH and oxidative conditions to copolymers, with a broad range of responses.

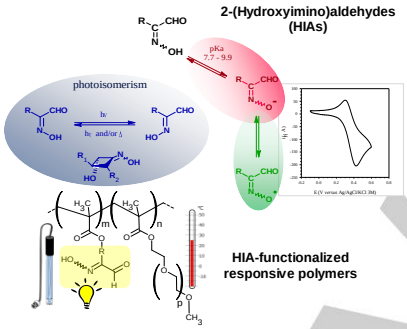

Prof. Patrizia Gentili, Dr. Martina Nardi, Irene Antignano, Dr. Paolo Cambise, Prof. Marco D'Abramo, Dr. Francesca D'Acunzo*, Dr. Alessandro Pinna, Dr. Emanuele Ussia*

Page No. – Page No.

2-(Hydroxyimino)aldehydes: Photochemical and Physico-Chemical Properties of a versatile functional group for monomer design

[1] M. Nardi, F. D'Acunzo, M. Clemente, G. Proietti, P. Gentili, *Polymer Chemistry* **2017**, *8*, 4233.

[2] K. Sugamoto, Y. Hamasuna, Y. I. Matsushita, T. Matsui, *Synlett* **1998**, 1270.

[3] T. L. Gilchrist, T. G. Roberts, *Journal of the Chemical Society, Perkin Transactions 1* **1983**, 1283.

[4] M. Baidya, H. Yamamoto, *Journal of the American Chemical Society* **2011**, *133*, 13880.

[5] P. Gentili, S. Pedetti, *Chemical Communications* **2012**, *48*, 5358.

[6] E. Abele, R. Abele, *Current Organic Synthesis* **2014**, *11*, 403.

[7] Y. Ashani, I. Silman, Hydroxylamines and Oximes: Biological Properties and Potential uses as Therapeutic Agents, in *The Chemistry of Hydroxylamines, Oximes and Hydroxamic Acids*, John Wiley & Sons, Ltd, **2008**, pp. 609.

[8] D. K. Kölmel, E. T. Kool, *Chemical Reviews* **2017**, *117*, 10358.

[9] K. K.-Y. Kung, K.-F. Wong, K.-C. Leung, M.-K. Wong, *Chemical Communications* **2013**, *49*, 6888.

[10] A. Balamurugan, H. I. Lee, *Macromolecules* **2015**, *48*, 3934.

[11] N. Singh, Y. Karpichev, A. K. Tiwari, K. Kuca, K. K. Ghosh, *Journal of Molecular Liquids* **2015**, *208*, 237.

[12] M. A. Gordillo, M. Soto-Monsalve, C. C. Carmona-Vargas, G. Gutiérrez, R. F. D'Vries, J. M. Lehn, M. N. Chaur, *Chemistry - A European Journal* **2017**, *23*, 14872.

[13] A. R. Hajipour, M. Karimzadeh, S. Jalilvand, H. Farrokhpour, A. N. Chermahini, *Computational and Theoretical Chemistry* **2014**, *1045*, 10.

[14] Y. A. Gur'eva, O. A. Zalevskaya, L. L. Frolova, I. N. Alekseev, P. A. Slepukhin, A. V. Kuchin, *Russian Journal of General Chemistry* **2014**, *84*, 137.

[15] A. V. Afonin, I. A. Ushakov, D. V. Pavlov, A. V. Ivanov, A. b. I. Mikhaleva, *Magnetic Resonance in Chemistry* **2010**, *48*, 685.

[16] V. A. Pavlov, J. A. S. Smith, T. A. Zjablikova, *Magnetic Resonance in Chemistry* **1992**, *30*, 716.

[17] D. S. Bohle, Z. Chua, I. Perepichka, K. Rosadiuk, *Chemistry - A European Journal* **2013**, *19*, 4223.

[18] M. A. M. Al-Alwani, A. B. Mohamad, N. A. Ludin, A. A. H. Kadhum, K. Sopian, *Renewable and Sustainable Energy Reviews* **2016**, *65*, 183.

[19] L. Infantes, S. Motherwell, Prediction of H-bonding motifs for pyrazoles and oximes using the Cambridge structural database, in *Science of Crystal Structures: Highlights in Crystallography*, **2015**, pp. 269.

[20] D. S. Bolotin, N. A. Bokach, V. Y. Kukushkin, *Coordination Chemistry Reviews* **2016**, *313*, 62.

[21] A. S. Dinca, C. Maxim, B. Cojocaru, F. Lloret, M. Julve, M. Andruh, *Inorganica Chimica Acta* **2016**, *440*, 148.

[22] L. Croitor, E. B. Coropceanu, A. E. Masunov, H. J. Rivera-Jacquez, A. V. Siminel, V. I. Zelentsov, T. Y. Datsko, M. S. Fonari, *Crystal Growth and Design* **2014**, *14*, 3935.

[23] a) D. R. Klaus, M. Keene, S. Silchenko, M. Berezin, N. Gerasimchuk, *Inorganic Chemistry* **2015**, *54*, 1890; b) A. Mann, N. Gerasimchuk, S. Silchenko, *Inorganica Chimica Acta* **2016**, *440*, 118.

[24] F. Wu, X. Tang, L. Guo, K. Yang, Y. Cai, *Soft Matter* **2013**, *9*, 4036.

[25] T. S. V. Buys, H. Cerfontain, J. A. J. Geenevasen, *Recueil des Travaux Chimiques des Pays‐Bas* **1990**, *109*, 531.

[26] G. A. Molander, J. A. C. Romero, *Tetrahedron* **2005**, *61*, 2631.

[27] A. De Mico, R. Margarita, L. Parlanti, A. Vescovi, G. Piancatelli, *Journal of Organic Chemistry* **1997**, *62*, 6974.

[28] J. Hu, D. L. Mattern, *Journal of Organic Chemistry* **2000**, *65*, 2277.

[29] M. G. Bell, R. A. Doti, M. J. Genin, P. A. Lander, T. Ma, P. R. Manninen, J. M. Ochoada, F. Qu, L. S. Stelzer, R. E. Stites, Fxr agonists, Patent WO 2007140183 A1, **2007.**

[30] H. D. Roth, Ligh-induced chemistry of oximes and derivatives, in *PATAI'S Chemistry of Functional Groups*, John Wiley & Sons, Ltd, **2010**.

[31] M. Cyman, J. Wielińska, H. Myszka, D. Trzybiński, A. Sikorski, A. Nowacki, B. Liberek, *Journal of Molecular Structure* **2016**, *1125*, 558.

[32] F. Blanco, I. Alkorta, J. Elguero, *Croatica Chemica Acta* **2009**, *82*, 173.

[33] F. Stunnenberg, H. Cerfontain, R. B. Rexwinkel, *Recueil des Travaux Chimiques des Pays ‐ Bas* **1992**, *111*, 438.

[34] D. E. Fast, A. Lauer, J. P. Menzel, A. M. Kelterer, G. Gescheidt, C. Barner-Kowollik, *Macromolecules* **2017**, *50*, 1815.

[35] T. S. V. Buys, H. Cerfontain, J. A. J. Geenevasen, F. Stunnenberg, *Recueil des Travaux Chimiques des Pays ‐ Bas* **1986**, *105*, 188.

[36] M. Oelgemöller, N. Hoffmann, *Organic and Biomolecular Chemistry* **2016**, *14*, 7392.

[37] a) D. Robertson, J. F. Cannon, N. Gerasimchuk, *Inorganic Chemistry* **2005**, *44*, 8326; b) O. T. Ilkun, S. J. Archibald, C. L. Barnes, N. Gerasimchuk, R. Biagioni, S. Silchenko, O. A. Gerasimchuk, V. N. Nemykin, *Dalton Transactions* **2008**, 5715; c) P. Baas, H. Cerfontain, *Journal of the Chemical Society, Perkin Transactions 2* **1979**, 156.

[38] D. Eddings, C. Barnes, N. Gerasimchuk, P. Durham, K. Domasevich, *Inorganic Chemistry* **2004**, *43*, 3894.

[39] G. K. Pierens, *Journal of Computational Chemistry* **2014**, *35*, 1388.

[40] P. Baas, H. Cerfontain, *Tetrahedron Letters* **1978**, *19*, 1501.

[41] Y. Zhang, H.-b. Fa, B. He, C.-j. Hou, D.-q. Huo, T.-c. Xia, W. Yin, *Journal of Solid State Electrochemistry* **2017**, *21*, 2117.

[42] S.-S. Chong, Y. Fu, L. Liu, Q.-X. Guo, *The Journal of Physical Chemistry A* **2007**, *111*, 13112.

[43] Y.-R. Luo, *Handbook of Bond Dissociation Energies in Organic Compounds*, CRC Press, **2007**.

[44] a) D. A. Pratt, J. A. Blake, P. Mulder, J. C. Walton, H. G. Korth, K. U. Ingold, *Journal of the American Chemical Society* **2004**, *126*, 10667; b) R. Dao, X. Wang, K. Chen, C. Zhao, J. Yao, H. Li, *Physical Chemistry Chemical Physics* **2017**, *19*, 22309.

[45] E. P. Friis, J. E. T. Andersen, L. L. Madsen, N. Bonander, P. Moller, J. Ulstrup, *Electrochimica Acta* **1998**, *43*, 1114.

[46] a) M. Yasuda, *Bulletin of the Chemical Society of Japan* **1959**, *32*, 429; b) T. Shedlovsky, R. Kay, The behaviour of carboxylic acids in mixed solvents, in *Electrolytes*, Pergamon Press, New York, **1962**, pp. 146.

[47] G. W. T. M. J. Frisch, H. B. Schlegel, G. E. Scuseria, M. A. Robb, J. R. Cheeseman, G. Scalmani, V. Barone, B. Mennucci, G. A. Petersson, H. Nakatsuji, M. Caricato, X. Li, H. P. Hratchian, A. F. Izmaylov, J. Bloino, G. Zheng, J. L. Sonnenberg, M. Hada, M. Ehara, K.Toyota, R. Fukuda, J. Hasegawa, M. Ishida, T. Nakajima, Y. Honda, O. Kitao, H. Nakai, T. Vreven, J. A. Montgomery, Jr., J.

E. Peralta, F. Ogliaro, M. Bearpark, J. J. Heyd, E. Brothers, K. N. Kudin, V. N. Staroverov, R. Kobayashi, J. Normand, K. Raghavachari, A. Rendell, J. C. Burant, S. S. Iyengar, J. Tomasi, M. Cossi, N. Rega, J. M. Millam, M. Klene, J. E. Knox, J. B. Cross, V. Bakken, C. Adamo, J. Jaramillo, R. Gomperts, R. E. Stratmann, O. Yazyev, A. J. Austin, R. Cammi, C. Pomelli, J. W. Ochterski, R. L. Martin, K. Morokuma, V. G. Zakrzewski, G. A. Voth, P. Salvador, J. J. Dannenberg, S. Dapprich, A. D. Daniels, O. Farkas, J. B. Foresman, J. V. Ortiz, J. Cioslowski, and D. J. Fox, *Gaussian 09, Revision A.02* **2009**.

[48] a) M. W. Lodewyk, M. R. Siebert, D. J. Tantillo, *Chemical Reviews* **2012**, *112*, 1839; b) M. W. Lodewyk, C. Soldi, P. B. Jones, M. M. Olmstead, J. Rita, J. T. Shaw, D. J. Tantillo, *Journal of the American Chemical Society* **2012**, *134*, 18550; c) M. W. Lodewyk, D. J. Tantillo, *Journal of Natural Products* **2011**, *74*, 1339; d) R. Jain, T. Bally, P. R. Rablen, *The Journal of Organic Chemistry* **2009**, *74*, 4017; e) P. R. Rablen, S. A. Pearlman, J. Finkbiner, *The Journal of Physical Chemistry A* **1999**, *103*, 7357.

[49] F. G. Bordwell, G. Z. Ji, *Journal of Organic Chemistry* **1992**, *57*, 3019.